



Published in final edited form as:

J Biomed Mater Res A. 2012 June ; 100(6): 1375–1386. doi:10.1002/jbm.a.34104.

The effects of substrate stiffness on the *in vitro* activation of macrophages and *in vivo* host response to poly(ethylene glycol)-based hydrogels

Anna K. Blakney, Mark D. Swartzlander, and Stephanie J. Bryant*

Department of Chemical & Biological Engineering, University of Colorado, Boulder, CO, USA

Anna K. Blakney: Anna.Blakney@colorado.edu; Mark D. Swartzlander: Mark.Swartzlander@colorado.edu

Abstract

Poly(ethylene glycol) (PEG) hydrogels, modified with RGD, are promising platforms for cell encapsulation and tissue engineering. While these hydrogels offer tunable mechanical properties, the extent of the host response may limit their *in vivo* applicability. The overall objective was to characterize the effects of hydrogel stiffness on the *in vitro* macrophage response and *in vivo* host response. We hypothesized that stiffer substrates induce better attachment, adhesion and increased cell spreading, which elevates the macrophage classically activated phenotype and leads to a more severe foreign body reaction (FBR). PEG-RGD hydrogels were fabricated with compressive moduli of 130, 240 and 840kPa, and the same RGD concentration. Hydrogel stiffness did not impact macrophage attachment, but elicited differences in cell morphology. Cells retained a round morphology on 130kPa substrates, with localized and dense F-actin and localized α_V integrin stainings. Contrarily, cells on stiffer substrates were more spread, with filopodia protruding from the cell, a more defined F-actin, and greater α_V integrin staining. When stimulated with lipopolysaccharide, macrophages had a classical activation phenotype, with increased expression of TNF- α , IL-1 β , and IL-6, however the degree of activation was significantly reduced with the softest hydrogels. A FBR ensued in response to all hydrogels when implanted subcutaneously in mice, but 28 days post-implantation the layer of macrophages at the implant surface was significantly lower in the softest hydrogels. In conclusion, hydrogels with lower stiffness led to reduced macrophage activation and a less severe and more typical FBR, and therefore are more suited for *in vivo* tissue engineering applications.

Keywords

Poly(ethylene glycol); hydrogel; macrophage/ monocyte; foreign body reaction; RGD

INTRODUCTION

Poly(ethylene glycol) (PEG)-based hydrogels formed from PEG di(meth)acrylate macromer precursors are a promising platform for cell-based tissue engineering applications. They present a ‘blank slate,’ which can be functionalized with biological moieties in a controlled and systematic manner creating environments that are specific for the tissue engineering application.¹ Through simple manipulations in the formulation, such as changes in macromer molecular weight or macromer concentration a wide range of material properties can be obtained.² Because of the ease by which these materials can be tuned, PEG-based hydrogels are being investigated for numerous tissue engineering applications that range

*Corresponding author: Stephanie J. Bryant: Stephanie.Bryant@colorado.edu.

from soft tissues (e.g. vasculature,³ nerve,⁴ and muscle⁵) to hard tissues (e.g. cartilage^{6,7} and bone^{8,9}).

While the nature of synthetic materials offer tunability, they may present challenges for *in vivo* applications. It is well known that when a non-biological material is implanted, the normal course of wound healing is altered and a foreign body reaction (FBR) ensues. The FBR is thought to be a series of cell-material surface-mediated interactions. It begins with non-specific protein adsorption followed by macrophage recruitment, attachment to the biomaterial, and activation.^{10,11} Activated macrophages are thought to orchestrate the FBR by secreting a number of molecules that are involved in inflammation, degradation of the foreign object and surrounding tissue, and recruiting non-inflammatory cells which eventually lead to the formation of a fibrous capsule.^{12,13} While macrophage activation may subside to a certain degree once a capsule is formed, macrophages can persist for the lifetime of the implant.¹⁴ From a tissue engineering perspective, the persistent presence of macrophages and their release of cytokines and reactive oxygen and nitrogen species may impact the cells within the scaffold and the developing tissue leading to apoptosis and/or inhibition/degradation of the neotissue. The fibrous capsule, which is typically avascular and dense, may act as a barrier between the scaffold and the host impacting integration of the engineered tissue with host tissue. While the fibrous capsule and associated macrophages/foreign body giant cells will eventually disappear once the synthetic material has degraded, the effects of the FBR may be long lasting.

We recently demonstrated that PEG-based hydrogels formed from PEG diacrylate precursors indeed elicit a FBR when implanted subcutaneously in immunocompetent mice.^{15,16} A strong early inflammatory reaction, characterized by a large band of macrophages at the hydrogel surface, ensues within two days post-implantation along with elevated levels of interleukin-1 β expression in the cells at and near the implant interface. This reaction persists throughout the four weeks, with little sign of stabilization. While PEG itself resists protein adsorption,¹⁷ PEG hydrogels formed from PEG-diacrylate are comprised of polyacrylate kinetic chains that are crosslinked by PEG. The kinetic chains confer some degree of hydrophobicity and may lead to nonspecific protein adsorption, thus eliciting a FBR. The incorporation of a biologically active molecule into the PEG hydrogel, specifically the cell adhesion moiety RGD, led to significant improvements in the reduction of macrophage activation as seen *in vitro* and the FBR *in vivo*, although a FBR still ensued. These findings suggest that while the FBR can be attenuated to a certain degree, additional studies are necessary to better understand the FBR to PEG-based hydrogels in order to realize their full *in vivo* potential.

We know that the FBR occurs when nearly all non-biological materials are implanted, but its severity depends on numerous factors, such as material chemistry¹⁸ and topography.¹⁹ Therefore in developing tissue scaffolds, the design choices may ultimately impact how the host responds to the scaffold once implant. One design choice that has gained considerable attention in recent years is substrate rigidity.^{20,21} The stiffness of the underlying substrate has been shown to have a significant impact on numerous cells and their fate, such as cellular cytoskeleton rearrangement,²² cell migration,²³ stem cell differentiation²¹, and muscle cell contractility.^{24,25} However, there is little known regarding how stiffness impacts macrophages and more specifically their activation and ultimately the FBR. Beningo *et al.*²⁶ reported that macrophages bind both stiff and soft particles to their cell membrane, but only readily phagocytose stiff particles, leading to more frustrated phagocytes. Fereol *et al.*²⁷ reported that macrophage cell spreading and cytoskeleton stress were higher on stiffer substrates. These reports provide evidence that macrophages indeed sense the stiffness of a substrate, implying that stiffness may play a role in the FBR.

Therefore, the overall objective for this study was to characterize the effects of hydrogel stiffness on macrophage interrogation by their attachment, adhesion, and activation *in vitro* and the FBR *in vivo*. We hypothesized that stiffer substrates would induce better attachment and adhesion and increased cell spreading, which would ultimately elevate the macrophage classically activated phenotype and lead to a more severe FBR *in vivo*. We chose to employ PEG hydrogels with RGD tethers, as we have shown that RGD reduces the severity of the FBR to PEG hydrogels, and the RGD tethers provide a mechanism by which macrophages, directly interacting with the hydrogel, can sense substrate stiffness via integrin-mediated events.²⁸ To isolate the effects of substrate stiffness, hydrogels were formed with varying stiffness, but with same concentration of RGD. *In vitro*, macrophage attachment, adhesion and activation were assessed where the latter was evaluated by probing macrophage phenotype across the spectrum of activation (i.e. classical, wound-healing and regulatory states).²⁹ PEG-RGD hydrogels were also implanted subcutaneously into immunocompetent mice for four weeks, and then analyzed for macrophage presence at the interface and fibrous capsule formation. Our findings support our hypothesis demonstrating that macrophages indeed sense their underlying substrate and that stiffer substrates lead to a more severe FBR.

MATERIAL AND METHODS

Hydrogel preparation

Poly(ethylene glycol) diacrylate (PEG-dA) was synthesized by reacting acryloyl chloride (Sigma-Aldrich) and triethylamine (Sigma-Aldrich) with poly(ethylene glycol) (3000 Da, PEG, Fluka) in dry toluene. Acryloyl chloride was added drop wise into a solution of PEG and TEA in excess toluene. The final molar ratio was 1 mol PEG to 4 mol triethylamine to 4.4 mol acryloyl chloride and the solution was reacted overnight at room temperature. PEG-dA product was purified by repeated precipitation in diethyl ether. The degree of acrylate substitution was determined by ¹H NMR to be greater than 95%.

Monoacrylated poly(ethylene glycol)- tyrosine-arginine-glycine-aspartic acid-serine (YRGDS) was synthesized as described previously.¹⁶ Briefly, 1 mol monoacrylate poly(ethylene glycol) N-hydroxysuccinimide (3400 Da, Laysan Bio) was reacted with 1.5 mol YRGDS (Genscript) oligopeptide in a 50 mM sodium bicarbonate buffer at pH of 8.4 for 2 hours. The monoacrylated PEG-YRGDS product was purified by dialysis, lyophilized, and stored under argon at 4°C. The extent of conjugation of the peptide to monoacrylated PEG was determined to be 90% by ¹H-NMR.

PEG-RGD hydrogels were formed by photopolymerization of a 10%, 20% or 40% (w/w) PEG-dA solution with 0.05% (w/w) photoinitiator (I2959, Irgacure, Ciba Specialty Chemical) with 2.5 mM monoacrylated PEG-YRGDS between two glass slides with 0.8mm spacers under 365 nm ultraviolet light (5–10 mW cm⁻²) for 10 min. All hydrogels were prepared under sterile conditions. All materials were rinsed three times in 70% ethanol overnight to sterilize the hydrogels, followed by four rinses in sterile phosphate buffered saline. Hydrogel sheets were punched into 5 mm disks.

Hydrogel Properties

PEG-RGD hydrogels were allowed to equilibrate for 24 hours prior to testing. The tangent modulus was determined from the linear region of the stress-strain curves of hydrated hydrogels subjected to unconfined compression applied at a rate of 0.5 mm/minute up to 15% strain (Synergie 100, 10 N; MTS). The equilibrium mass swelling ratio (m_s/m_d) was determined from the swollen wet weight (m_s) and the dry polymer weight (m_d).

Macrophage culture

For experiments investigating cell attachment and morphology, RAW 264.7 macrophages (American Type Cell Culture) were used. Macrophages suspended in Dulbecco's modified Eagle medium (DMEM) (Mediatech) supplemented with penicillin/streptomycin/fungizone (PSF) (Invitrogen) were seeded on top of PEG-RGD hydrogels at a concentration of 2.5×10^4 cells per gel for cell attachment studies and 5.0×10^4 cells per gel for morphology studies. Cells were allowed to attach for two hours after which the medium was replaced with DMEM supplemented with 10% fetal bovine serum (FBS, Atlanta Biological) and PSF.

For experiments investigating gene expression, primary bone marrow derived murine monocytes were isolated from 6-week-old male c57bl/6 mice (Charles River Laboratories) as described previously by Jay *et al.*³⁰ Briefly, bone marrow was flushed from tibias and femurs with Iscove's modified Dulbecco's medium (IMDM) (Invitrogen). Bone marrow isolates were suspended in IMDM with 10% FBS and PSF. The cell suspension was layered over Lympholyte M (Accurate Chemicals) and centrifuged per manufacturer's instruction and the portion containing mononuclear cells collected. The cells were resuspended at 10^6 cells ml^{-1} in expansion medium (IMDM + 20% FBS, 2 mM l-glutamine, PSF, 1.5 ng ml^{-1} human macrophage colony stimulating factor (R&D systems) and 100 ng ml^{-1} huFLT-3 (R&D systems)), plated at 1.7×10^5 cells cm^{-2} in 100 mm Petri dishes and cultured to confluency (10 days) prior to use in the experiments. Cells were seeded onto the PEG-RGD hydrogels at a density of 5×10^4 cells per hydrogel in serum-free medium (IMDM and PSF) and allowed to adhere for 6 hours. The medium was then replaced with medium with serum (IMDM + 10% FBS, PSF) and the cells were cultured for an additional 18 hours. A subset of samples were removed from culture and prepared for gene expression analysis. For the remainder of the samples, the medium was exchanged with medium supplemented with $1 \mu\text{g ml}^{-1}$ LPS from *E. coli* (Sigma-Aldrich). This concentration was chosen because it has been shown to stimulate pro-inflammatory cytokine expression in macrophages *in vitro*.^{31,32} Samples were removed from culture and prepared for gene expression analysis.

Macrophage Attachment and Morphology

RAW 264.7 cells which were cultured for 24 hours were either fixed in 4% paraformaldehyde and then stored in 15% sucrose solution or lysed in a solution of 20 mM TRIS, 2 mM EDTA, 150 mM NaCl and 0.5% Triton X-100 in deionized water. A subset of the fixed samples ($n=4$) were permeabilized with Triton X-100, and stained with AlexaFluor 488 phalloidin (1:30, Invitrogen) with 1% BSA. The other set ($n=4$) was permeabilized with Triton X-100, blocked, treated anti-integrin α_V primary antibody (1:30, rabbit polyclonal IgG, Santa Cruz Biotechnology) overnight at 4°C , followed by treatment with secondary antibody (1:30, Goat anti-rabbit IgG AlexaFluor 488, Invitrogen). All samples were counterstained with DAPI, a nucleic acid stain (Molecular Probes, 300nM) and then imaged via confocal microscopy (Zeiss LSM5 Pascal). The lysed samples ($n=4$) were assayed by PicoGreen® (Invitrogen) per manufacturer to determine the total amount of dsDNA, which was used as a measure of cell attachment.

RNA isolation and real-time reverse transcription polymerase chain reaction

At prescribed time points, macrophages adhered to hydrogels disks ($n=4$) were lysed using TRK lysis buffer (Omega) and RNA isolated using an E.Z.N.A microelute kit (Omega) per the manufacturer's instructions. The purity and quantity of RNA was determined using a Nanodrop instrument (ND-1000, Thermo Scientific) with A260/280 greater than 1.90. Purified RNA was reverse transcribed to cDNA using a High Capacity cDNA Reverse Transcription Kit (Applied Biosystems) and samples stored at -80°C until PCR analysis was performed. RT-PCR was performed with Fast SYBR Green Master Mix (Applied Biosystems) with the 7500 Fast system (Applied Biosystems). Custom primers were

designed using Primer Express 3.0 software (Applied Biosystems) and validated for both efficiency and stability of the house-keeping gene L32, which encodes a ribosomal protein. The primer sequences for tumor necrosis factor- α (TNF- α), interleukin-1 β (IL-1 β), interleukin-6 (IL-6), interleukin-10 (IL-10), and Arginase I and L32 were used as previously listed^{15,16} with efficiencies of 2.09, 1.91, 1.99, 1.90 and 1.95, respectively. The sequence for IL-6 is Forward: 5'-TCGGAGGCTTAATTACACATGTTC-3' and Reverse: 5'-TGCCATTGCACAACCTTTTTTC T-3' with an efficiency of 2.05. The data are presented as relative expression (RE) or normalized expression (NE):

$$RE = \frac{E_{HKG}^{C_t}}{E_{GOI}^{C_t}} \quad NE = \frac{E_{HKG}^{C_{t,calibrator}-C_{t,sample}}}{E_{GOI}^{C_{t,calibrator}-C_{t,sample}}}$$

where E is the primer efficiency, HKG is the house-keeping gene, GOI is the gene of interest, C_t is the cycle number where the sample crosses the threshold and the calibrator is the time when LPS was administered, referred to as time zero hour.

Implantation study

Prior to implantation, all hydrogels were confirmed to be free of endotoxins. Hydrogels were implanted into dorsal subcutaneous pockets on six- to eight-week-old, male c57bl/6 mice. One pocket was formed over each shoulder and hip for a total of four pockets per animal. One construct of PEG-RGD (10%, 20% or 40% (w/w) PEG-dA) was placed into a single pocket, in a random order. The incisions were closed with surgical staples. Animals were monitored daily for any abnormalities at the wound site. Mice were sacrificed at 28 days post-implantation by CO₂ asphyxiation and cervical dislocation. Implants were excised with surrounding tissue and processed for (immuno)histological analysis (n=6).

(Immuno)histological analysis

Explants were fixed in 4% paraformaldehyde immediately for 24 hours after extraction. Paraformaldehyde was replaced with 15% sucrose and the explants were stored at 4°C until staining. Dehydration and paraffin embedding were carried out with standard protocols. Sections (10 μ m) were stained with Masson's Trichrome following standard protocols.

Immunohistochemical staining was also carried out for detection of the Mac3 antigen, a marker specific to tissue activated macrophages.³³ Briefly, tissue sections were deparaffinized, blocked and incubated with rat anti-mouse Mac3 primary antibodies (BD Biosciences) at a 1:20 dilution followed by a biotinylated anti-rat secondary antibody (BD Biosciences) at a 1:30 dilution. The samples were subsequently treated with Steptavidin-HRP (BD Biosciences) and counterstained with methyl green (Vector Labs).

All tissue sections were imaged using light microscopy (Zeiss, Axioskop 40) with 10, 20, or 40x objectives with a digital camera (Diagnostic Instruments, MN 14.2 Color Mosaic) using SPOT Software v. 4.6. Inflammatory cells were evaluated semi-quantitatively using NIH ImageJ software by measuring the thickness of the inflammatory cell layer at the implant surface.

Statistical analysis

One-way analysis of variance was performed using KaleidaGraph software for semi-quantitative analysis of histological samples and relative gene expression, for each material type. Two-way analysis of variance was performed using MiniTab 16 software for normalized gene expression for reach material type, with time and gel stiffness as factors.

Pair-wise comparisons were carried out using Tukey's post-hoc test with an α of 0.05. A p value of 0.05 was used to determine statistical significance. All data are presented as means \pm standard deviation.

IACUC approval

NIH guidelines for the care and use of laboratory animals (NIH Publication #85-23 Rev. 1985) have been observed. All animal protocols were approved by the University of Colorado at Boulder Institutional Animal Care and Use Committee.

RESULTS

Hydrogels properties

PEG hydrogels were formed from different concentrations of PEG-dA (10, 20 and 40% (w/w) in solution prior to polymerization), but each with the same total amount of RGD to produce hydrogels with a low, medium and high degree of relative crosslinking. The resulting PEG-RGD hydrogel properties are given in Table 1. The tangent modulus under compression increased with increasing PEG-dA concentration with values of 130, 240 and 840 kPa. The equilibrium swelling ratio decreased with increasing PEG-dA concentration with values that ranged from 4.6 to 10.

In vitro macrophage attachment and morphology

RAW 246.7 macrophages were used to determine whether hydrogel stiffness impacted macrophage attachment or morphology. After 24 hours, macrophage density was similar among all three hydrogel substrates, as measured by total DNA content. This finding indicates that substrate stiffness was not a factor in macrophage attachment.

Macrophage morphology after attachment to the constructs was observed after 48 hours using α_V integrin staining as well as phalloidin staining to visualize the actin filaments. The α_V staining indicated less spreading of the cells and a more localized attachment, presumably to RGD tethers, near the nucleus of the cell on the softest substrates. For the 240 and 840 kPa hydrogels, the integrin is visibly more present throughout the cell when compared to cells on the 130 kPa hydrogel. The F-actin organization also exhibited visual differences as a function of substrate stiffness. For the 130 kPa substrate, cells were rounded, compact and the actin was centralized around the nucleus. Macrophages on the 240 kPa substrate were more spread, exhibiting extended branches of actin, which was more defined throughout the cell. Finally, cells on the 840 kPa substrate had the greatest degree of spreading evidenced by greater staining for actin in a given cell in a given plane of view with a myriad of highly extended branches.

In vitro macrophage response to PEG-RGD hydrogels

Initially, macrophage phenotype in response to PEG-RGD hydrogels of varying substrate stiffness in the absence of any inflammatory co-stimulants was assessed. Primary bone marrow derived murine macrophages were cultured on PEG-RGD hydrogels for 24 hours and their mRNA evaluated by quantitative RT-PCR for genes which cover the spectrum of macrophage activation. Relative expression is given in Figure 2 and the results from a one-way analysis of variance with gel stiffness as a factor is shown in Table 2. The genes evaluated for their close association with inflammation were TNF- α , IL-1 β , and IL-6. For all genes, mean relative expression values decreased with increasing hydrogel stiffness but this decrease was only significant for IL-1 β and between 130 and 840 kPa gels ($p=0.0356$). IL-10 was evaluated for its close association with immunoregulation, but its expression was not affected by substrate stiffness. Lastly, Arginase I was evaluated for its close association

with wound healing. Mean relative expression values for Arginase I expression were highest for the 240 kPa gels, but not significantly.

Macrophage response to PEG-RGD hydrogels when stimulated with LPS

Macrophage phenotype in response to PEG-RGD hydrogels of varying substrate stiffness in the presence of LPS was assessed. Primary bone marrow derived murine macrophages were cultured on PEG-RGD hydrogels for 4, 8 or 24 hours in the presence of LPS and their mRNA evaluated by quantitative RT-PCR for genes which cover the spectrum of macrophage activation. Normalized gene expression is given in Figure 3 the results from a two-way analysis of variance with culture time and gel stiffness as factors is shown in Table 3. For the genes closely associated with inflammation (TNF- α , IL-1 β , and IL-6) culture time and stiffness were significant factors affecting their expression. All three genes were elevated with LPS stimulation. In general, IL-1 β and IL-6 expressions were highest for the 840 kPa gels when compared to the 130 and 240 kPa gels. For example, at 24 hours IL-1 β and IL-6 expressions for the 840 kPa gels were 2-fold ($p < 0.0001$) and 4.5-fold ($p = 0.0001$) higher than the 130 kPa gels, respectively and 1.4-fold ($p = 0.0364$) and 6.5-fold ($p < 0.0001$) higher than the 240 kPa gels. For IL-10 expression, culture time ($p < 0.0001$) and hydrogel stiffness ($p < 0.0001$) were both factors affecting its expression. At 24 hours, IL-10 expression for the 840 kPa gel was 2.6-fold ($p = 0.0004$) higher than the 130 kPa gels. For Arginase I expression, culture time and hydrogel stiffness were not significant factors. However, there were significant differences at the 24 hour time point which are worth noting. At 24 hours, the 130 kPa gel had 150-fold higher ($p = 0.0474$) expression over the 840 kPa gels.

In vivo host response to PEG-RGD hydrogels

The foreign body reaction to subcutaneously implanted PEG-RGD hydrogels of each stiffness, 130, 240 and 840 kPa, was investigated 28 days post-implantation. Representative histological micrographs of sections stained by Masson's Trichrome to assess collagen deposition and fibrous capsule formation and for the macrophage specific cell surface marker, Mac3 (CD107b), which stains activated tissue macrophages, are shown in Figure 4. Qualitatively, hydrogel stiffness led to gross differences in the host response to the PEG-RGD hydrogels.

The 130 kPa gels were surrounded by a thin layer of densely packed inflammatory cells at the implant surface on both the dorsal and ventral sides. Just beyond this cell layer was evidence of a fairly dense thin fibrous capsule comprised of non-inflammatory cells and collagen (Fig 4a,d,g). The dense capsule was surrounded by a more disorganized collagenous matrix. The cells at the implant surface were confirmed to be macrophages, by positive staining for Mac3 (Fig 4j). In general, there were more macrophages and a thicker fibrous capsule along the ventral side of the implant compared to the dorsal side.

A similar host reaction to the 130 kPa gel was seen for the 240 kPa gel, but the reaction was more severe. The 240 kPa gel was surrounded by a thick layer of densely packed inflammatory cells (Fig 4b,e,h), confirmed to be macrophages (Fig 4k). As compared to the 130 kPa gels, a thicker but less dense fibrous capsule comprised of non-inflammatory cells and collagen surrounded the implant. The fibrous capsule was surrounded by a more disorganized collagenous matrix. As seen with the 130 kPa gels, there were a greater number of macrophages and a thicker fibrous capsule along the ventral side of the implant when compared to the dorsal side for the 240 kPa gels.

With increasing stiffness, the severity of the FBR continued to worsen. The 840 kPa gels were surrounded by a large layer of inflammatory cells (Fig 4c,f,i), which were confirmed to

be activated macrophages (Fig 4I). The fibrous capsule surrounding the inflammatory cells along the dorsal side was similar to that observed for the 240 kPa gels. However, the ventral side formed a much more loose fibrous network of non-inflammatory cells with substantially less collagen. The fibrous capsule was surrounded by another collagenous matrix, which was more disorganized compared to the dorsal side capsule and more organized compared to the ventral side. As seen with the 130 kPa and 240 kPa gels, there were a greater number of macrophages and a thicker fibrous capsule along the ventral side of the implant when compared to the dorsal side for the 840 kPa gels.

Semi-quantitative analysis of the host reaction

To quantify the host reaction to each of the hydrogels, measurements were made of the layer of inflammatory cells immediately at the material interface (Fig. 5). After 28 days, the 130 kPa gels had the smallest layer of activated macrophages surrounding the implant, ~30 μm thick on the dorsal side and ~35 μm thick on the ventral side. The 240 kPa gel had a significantly thicker layer of macrophages ~74 μm thick on the dorsal side and ~139 μm thick on the ventral side ($p < 0.05$). The 840 kPa gels had the thickest layer of activated macrophages ~88 μm on the dorsal side and ~208 μm deep on the ventral side, which were significantly thicker than 130 kPa gels ($p < 0.05$), but not the 240 kPa gels. The layer of macrophages was consistently greater on the dorsal side compared to the ventral side for all gels. The formation of a fibrous capsule was apparent in all cases, although a defined boundary for the capsule was not always observed making it difficult to quantify the fibrous capsule layer. However, the general trend indicated a thicker fibrous capsule with the more stiff hydrogels.

DISCUSSION

The results presented in this study demonstrate that PEG-RGD hydrogels induce a classically activated macrophage phenotype *in vitro* when co-stimulated with lipopolysaccharide (LPS) and elicit a foreign body reaction *in vivo*, characterized by macrophage infiltration and fibrous capsule formation, but that the severity of the response strongly depends on hydrogel stiffness. Our main finding is that hydrogels with lower stiffness lead to reduced macrophage activation and a less severe and more typical FBR. This finding may in part be attributed to distinctly different cell morphologies that arose due to gel stiffness, as seen in the spatial localization of F-actin and integrin receptors.

Many tissue engineering strategies that use PEG hydrogels incorporate proteins or peptides to support cell adhesion and promote cell-material interactions.¹ We chose to investigate PEG hydrogels with RGD tethers for several reasons. RGD is the most widely studied cell adhesion peptide in tissue engineering^{34–36} and is easily incorporated into PEG hydrogels in a controlled and reproducible manner.³⁷ Our previous findings showed that RGD is able to attenuate, although not completely, the FBR to PEG hydrogels.^{15,16} Similarly, others have reported reduced inflammatory cytokine production by RGD-mediated binding events.^{38,39} In addition, RGD is conserved throughout many matricellular and extracellular matrix proteins to which macrophages can bind through several different integrin receptors.⁴⁰ Therefore, PEG-RGD hydrogels served as an excellent platform to which RGD concentration could be held constant, while independently varying hydrogel stiffness, enabling the effects of substrate stiffness on macrophages and the FBR to be probed.

The integrin pairs, $\alpha_5\beta_1$, $\alpha_v\beta_1$, and $\alpha_v\beta_3$, are well known integrin pairs that bind to RGD.⁴¹ However, previous studies have shown that macrophages when cultured on biomaterials express minimal α_5 subunits but substantial α_v subunits.⁴² Further studies have shown that β_1 not β_3 subunits are essential in RGD-mediated macrophage adhesion to biomaterials.^{43,44} Therefore, $\alpha_v\beta_1$ may be a prominent integrin pair mediating macrophage adhesion to RGD.

In this study, macrophages were seeded onto the PEG-RGD hydrogels in serum-free conditions in an effort to ensure that macrophages interacted directly with RGD rather than any secondary non-specific adsorbed protein. We confirmed that macrophages expressed the α_v subunit when cultured on all three PEG-RGD hydrogel substrates, suggesting that an α_v integrin binding pair, e.g. $\alpha_v \beta_1$, is one mechanism through which macrophages sense the PEG-RGD substrata. While the concentration of RGD was held constant, there were distinct differences in the integrin staining. Most notably, greater staining was observed in the stiffer substrates (240 and 840 kPa) when compared to the softer substrate, a finding that correlated with the increased cell spreading observed on the stiffer substrates. This result suggests that hydrogel stiffness mediated cell adhesion and subsequently reduced or altered the number and/or spatial location of integrin-ligand bonds, despite the similar presentation of RGD ligands.

To probe the effects of hydrogel stiffness on macrophage activation, we turned to *in vitro* experiments because they provided a more controlled environment for studying macrophages. During the initial culture period, hydrogel stiffness had minimal effects on macrophage phenotype, with one notable exception where IL-1 β expression was significantly affected by gel stiffness, and interestingly was lower in gels with increasing substrate stiffness. Others have recently reported reduced IL-1 β production by human monocyte/macrophages with increased cell spreading when cultured in the absence of an inflammatory stimulus.⁴⁵ To better capture the *in vivo* environment during the FBR, simulating an inflammatory environment was necessary.⁴⁶⁻⁴⁸ When activated by LPS, macrophages responded by phenotypic changes that were largely characteristic of a classically activated phenotype regardless of hydrogel stiffness, evidenced by elevated expression levels of the pro-inflammatory cytokines, TNF- α , IL-1 β , and IL-6, which remained elevated throughout the study. The level of expression of all three inflammatory cytokines was significantly impacted by gel stiffness and was lowest for the 130 kPa, indicating that the softest gel exhibited a reduced classically activated macrophage phenotype. IL-10 expression was also probed which is considered an immunoregulatory protein and a potent anti-inflammatory cytokine and has been implicated in the late stages of the FBR associated with its stabilization.⁴⁹ IL-10 expression was also elevated, and to a greater degree with increasing gel stiffness, but its peak appears to be delayed when compared to the pro-inflammatory cytokines. The last gene investigated was Arginase type I, which is up-regulated during wound healing by macrophages and is involved in the synthesis of collagen precursors. Arginase expression, while not significantly affected during the course of the experiment or by gel stiffness did show significantly higher levels at 24 hours for the 130 kPa over the 840 kPa gel. While we cannot draw definitive conclusions, these results suggest that the 130 kPa may shift the macrophages towards a wound healing phenotype, and perhaps more quickly than the macrophages on stiffer substrates. We have previously reported that macrophages after being stimulated by LPS shift to a wound healing phenotype but this shift was not apparent until 48 hours.⁵⁰ Taken together, our *in vitro* results demonstrate that in a simulated inflammatory environment, softer substrates help to reduce the classically activated macrophage phenotype and shift to a wound healing phenotype.

While our *in vitro* findings were insightful, the *in vivo* environment and the FBR is a complex series of highly coordinated events involving not only inflammatory cells but also non-inflammatory cells. Although simplistic, our *in vitro* results mirrored that of our more complex *vivo* findings, where softer hydrogels elicited an improved and less severe FBR. In fact, the improvements in the FBR with the softest hydrogel were quite remarkable. We previously reported that PEG-only hydrogels with no biological recognition and with properties resembling those of the 240 kPa gels, led to an atypical FBR characterized by a large number of macrophages persisting at the implant surface with no obvious signs of

stabilization by 28 days.¹⁵ The stiffest hydrogels investigated in this study, 840 kPa, exhibited a response that was similar to that of the PEG-only hydrogels with respect to the large macrophage presence at the material interface. However, there was evidence of a nascent fibrous capsule, which suggests that some degree of stabilizing occurred. The response was improved with 240 kPa and results were similar to that of our previous reports, but the FBR was still largely atypical.¹⁵ The softest hydrogels investigated in this study, however, exhibited a more typical FBR. The layer of macrophages surrounding the implant, while present (~35 μm), was substantially smaller when compared to the more stiff hydrogels and approached that of previously reported for medical grade silicone (~16 μm), a biomaterial that elicits a typical FBR.¹⁵ Furthermore, the FBR appeared to be largely stabilized by 28 days with a thin dense avascular fibrous capsule that was ~30–40 μm thick. This thickness is on par with those reported with other materials, such as expanded polytetrafluoroethylene,⁵¹ degradable polyester polyurethanes,⁵² polycaprolactone,⁵³ and polyethylene terephthalate.⁵⁴ Our *in vivo* findings further support our *in vitro* conclusions and support our hypothesis that softer hydrogels lead to a reduced FBR possible by attenuating macrophage activation at the host-hydrogel interface.

While we focus on hydrogel stiffness as the important external cue sensed by the macrophages, it is important to recognize the degree of hydrogel swelling, which is inversely related to the mechanical properties through crosslinking density, may also be playing a role particularly for the *in vivo* environment. Because hydrogels absorb many times their polymer weight in water, they form loosely crosslinked networks that allow for facile transport of water and other molecules through the gels. The hydrogels investigated in this study have water contents that range from 80% for the stiffest, most highly crosslinked gel to 90% for the softest and most loosely crosslinked gel. When these highly swollen hydrogels are implanted into a wound site, they may ‘soak up’ many of the proinflammatory cytokines that are present in the exudate at the early stages of a wound and subsequently lead to their prolonged presence and chronic inflammation. Because the more loosely crosslinked hydrogel shows a reduced FBR, it seems that this phenomenon is an unlikely contributor to the FBR.

It has been shown, for many cell types, that cells sense the stiffness of their substrata through integrin-mediated events involving focal adhesions, actin organization and development of stress fibers.^{55–57} The overwhelming observations are that the stiffer the substrate, the stronger the focal adhesions are and the more organized the stress fibers are. It is thought that the development of cellular prestress as a result of these events trigger a wide range of downstream events in the cell that have been implicated in morphogenesis, physiology and disease.⁵⁷ In this study, macrophage morphology and more specifically the localization of F-actin was dramatically different on the three substrates. On the softest substrates, 130 kPa, albeit not very soft in the context of many other cells, macrophages appeared to have a largely rounded morphology with few visible filopodia and a localized and dense F-actin structure. Contrarily on the stiffer substrates (240 and 840 kPa), the cells appeared more spread with evidence of filopodia protruding from the cell and a more defined F-actin. While the same general trends have been reported for contractile adherent cells, the morphology of the macrophages in response to their substrata stiffness is actually quite different. For contractile adherent cells, cells typically developed their F-actin into highly organized stress fibers as substrate stiffness increases but this transition occurs on substrates as soft as ~10 kPa.²¹ It has been shown that macrophages, as part of their myeloid lineage, do not possess stress fibers,⁵⁸ which may in large part be due to the fact that their interaction with their surrounding matrix, when not migrating, is not a key part of their innate function.²⁹ In this study, the F-actin on the stiffer substrates did not have an appearance that was more organized, although not characteristic of stress fibers. While macrophages may not have stress fibers, they have been shown to respond to substrate

stiffness by increasing their cytoskeletal stiffness, suggesting that macrophages may have a different set of cytoskeletal proteins surrounding F-Actin that are regulated in response to the substrate.²⁷ Interestingly, macrophages appear to be more sensitive to stiffer substrates, while contractile adherent cells tend to be less sensitive when substrates are stiff.⁵⁶ Taken together, our findings suggest that substrate stiffness likely through integrin-mediated events direct changes in macrophage morphology and cytoskeletal organization, which subsequently alters their reaction to the PEG-RGD hydrogels. When macrophages are more round, less spread with no obvious cytoskeletal organization, their activation appears to be reduced when compared to cells which are more spread with some cytoskeletal organization in an inflammatory environment. This reduced activation may have led to the improved FBR observed *in vivo*.

The exact mechanisms by which substrate stiffness drives macrophage activation remain to be elucidated. With recent evidence pointing towards a mechanism that is very different than most cells, additional studies are clearly warranted given the importance of the FBR in medical device failure⁵⁹ and that it will likely be a hurdle to regenerating tissues. Our findings have significant implications in tissue engineering strategies that utilize PEG-based hydrogels. Our findings suggest that employing softer hydrogels as scaffolds in cell-based tissue regeneration will help to minimize the negative effects that may arise as a result of the FBR. The softer hydrogels have also shown more promise with enhancing cell survival and extracellular matrix elaboration due to the larger mesh size, making them even more attractive.^{60–64} Overall, our findings indicate that stiffness of the synthetic scaffold will contribute to the severity of the FBR and is an external cue that should be considered when designing scaffolds for tissue engineering.

CONCLUSIONS

The results from this study support our hypothesis that stiffer PEG-RGD hydrogels lead to increased cell spreading with a more organized F-actin cytoskeleton network, although not to differences in cell attachment, to elevated expression levels characteristic of a macrophage classically activated phenotype, and to a more severe FBR *in vivo*. The murine model allowed for the direct comparison between *in vitro* and *in vivo* experiments, in which both environments showed similar results. Our results indicated stark differences in cell morphology as a result of hydrogel stiffness, which led to differences in the F-actin cytoskeletal structure and integrin localization. Because it is thought that cells sense their underlying substrate primarily through integrin-mediated events and changes in their cytoskeletal stress, our findings suggest that maintaining a more round morphology with localized integrin staining may be important to minimizing macrophage classical activation and reducing the number of inflammatory cells at the implant interface and the fibrous capsule.

Acknowledgments

Financial support for this project was provided by Award Number NIH 1R03DE019505, ARRA supplement to NIH K22DE016608 and NSF CAREER Award.

References

1. Tibbitt MW, Anseth KS. Hydrogels as Extracellular Matrix Mimics for 3D Cell Culture. *Biotechnology and Bioengineering*. 2009; 103(4):655–663. [PubMed: 19472329]
2. Peppas NA, Hilt JZ, Khademhosseini A, Langer R. Hydrogels in biology and medicine: From molecular principles to bionanotechnology. *Advanced Materials*. 2006; 18(11):1345–1360.

3. Moon JJ, Hahn MS, Kim I, Nsiah BA, West JL. Micropatterning of Poly(Ethylene Glycol) Diacrylate Hydrogels with Biomolecules to Regulate and Guide Endothelial Morphogenesis. *Tissue Engineering Part A*. 2009; 15(3):579–585. [PubMed: 18803481]
4. Mahoney MJ, Anseth KS. Three-dimensional growth and function of neural tissue in degradable polyethylene glycol hydrogels. *Biomaterials*. 2006; 27(10):2265–2274. [PubMed: 16318872]
5. Iyer RK, Chiu LLY, Radisic M. Microfabricated poly(ethylene glycol) templates enable rapid screening of triculture conditions for cardiac tissue engineering. *Journal of Biomedical Materials Research Part A*. 2009; 89A(3):616–631. [PubMed: 18442120]
6. Nicodemus GD, Bryant SJ. The role of hydrogel structure and dynamic loading on chondrocyte gene expression and matrix formation. *Journal of Biomechanics*. 2008; 41(7):1528–1536. [PubMed: 18417139]
7. Appelman TP, Mizrahi J, Elisseff JH, Seliktar D. The influence of biological motifs and dynamic mechanical stimulation in hydrogel scaffold systems on the phenotype of chondrocytes. *Biomaterials*. 2011; 32(6):1508–1516. [PubMed: 21093907]
8. Benoit DSW, Durney AR, Anseth KS. Manipulations in hydrogel degradation behavior enhance osteoblast function and mineralized tissue formation. *Tissue Engineering*. 2006; 12(6):1663–1673. [PubMed: 16846361]
9. Yang F, Williams CG, Wang DA, Lee H, Manson PN, Elisseff J. The effect of incorporating RGD adhesive peptide in polyethylene glycol diacrylate hydrogel on osteogenesis of bone marrow stromal cells. *Biomaterials*. 2005; 26(30):5991–5998. [PubMed: 15878198]
10. Anderson JM, Rodriguez A, Chang DT. Foreign body reaction to biomaterials. *Seminars in Immunology*. 2008; 20(2):86–100. [PubMed: 18162407]
11. Ratner BD, Bryant SJ. Biomaterials: Where we have been and where we are going. *Annual Review of Biomedical Engineering*. 2004; 6:41–75.
12. Anderson JM, Marchant R, Hiltner A, Suzuki S, Miller K. Biocompatibility and the inflammatory response. *Abstracts of Papers of the American Chemical Society*. 1983 Mar.185:99–POLY.
13. Anderson JM, Miller KM. Biomaterial biocompatibility and the macrophage. *Biomaterials*. 1984; 5(1):5–10. [PubMed: 6375747]
14. Anderson JM. Biological responses to materials. *Annual Review of Materials Research*. 2001; 31:81–110.
15. Lynn AD, Blakney AK, Kyriakides TR, Bryant SJ. Temporal progression of the host response to implanted poly(ethylene glycol)-based hydrogels. *Journal of Biomedical Materials Research Part A*. 2011; 96A(4):621–631. [PubMed: 21268236]
16. Lynn AD, Kyriakides TR, Bryant SJ. Characterization of the in vitro macrophage response and in vivo host response to poly(ethylene glycol)-based hydrogels. *Journal of Biomedical Materials Research Part A*. 2010; 93A(3):941–953. [PubMed: 19708075]
17. Jeon SI, Lee JH, Andrade JD, Degennes PG. Protein surface interactions in the presence of polyethylene oxide .1. Simplified theory. *Journal of Colloid and Interface Science*. 1991; 142(1): 149–158.
18. Schutte RJ, Parisi-Amon A, Reichert WM. Cytokine profiling using monocytes/macrophages cultured on common biomaterials with a range of surface chemistries. *Journal of Biomedical Materials Research Part A*. 2009; 88A(1):128–139. [PubMed: 18260130]
19. Chen SL, Jones JA, Xu YG, Low HY, Anderson JM, Leong KW. Characterization of topographical effects on macrophage behavior in a foreign body response model. *Biomaterials*. 2010; 31(13):3479–3491. [PubMed: 20138663]
20. Nemir S, West JL. Synthetic Materials in the Study of Cell Response to Substrate Rigidity. *Annals of Biomedical Engineering*. 2010; 38(1):2–20. [PubMed: 19816774]
21. Engler AJ, Sen S, Sweeney HL, Discher DE. Matrix elasticity directs stem cell lineage specification. *Cell*. 2006; 126(4):677–689. [PubMed: 16923388]
22. Ghosh K, Pan Z, Guan E, Ge SR, Liu YJ, Nakamura T, Ren XD, Rafailovich M, Clark RAF. Cell adaptation to a physiologically relevant ECM mimic with different viscoelastic properties. *Biomaterials*. 2007; 28(4):671–679. [PubMed: 17049594]
23. Lo CM, Wang HB, Dembo M, Wang YL. Cell movement is guided by the rigidity of the substrate. *Biophysical Journal*. 2000; 79(1):144–152. [PubMed: 10866943]

24. Engler AJ, Carag-Krieger C, Johnson CP, Raab M, Tang HY, Speicher DW, Sanger JW, Sanger JM, Discher DE. Embryonic cardiomyocytes beat best on a matrix with heart-like elasticity: scar-like rigidity inhibits beating. *Journal Of Cell Science*. 2008; 121(22):3794–3802. [PubMed: 18957515]
25. Bhana B, Iyer RK, Chen WL, Zhao R, Sider KL, Likhitanichkul M, Simmons CA, Radisic M. Influence of substrate stiffness on the phenotype of heart cells. *Biotechnology and Bioengineering*. 2010; 105(6):1148–60. [PubMed: 20014437]
26. Beningo KA, Lo CM, Wang YL. Flexible polyacrylamide substrata for the analysis of mechanical interactions at cell-substratum adhesions. *Methods in Cell-Matrix Adhesion*. 2002; 69:325–339.
27. Fereol S, Fodil R, Labat B, Galiacy S, Laurent VM, Louis B, Isabay D, Planus E. Sensitivity of alveolar macrophages to substrate mechanical and adhesive properties. *Cell Motility and the Cytoskeleton*. 2006; 63(6):321–340. [PubMed: 16634082]
28. Antonov AS, Antonova GN, Munn DH, Mivechi N, Lucas R, Catravas JD, Verin AD. alpha V beta 3 Integrin Regulates Macrophage Inflammatory Responses via PI3 Kinase/Akt-Dependent NF-kappa B Activation. *Journal of Cellular Physiology*. 2011; 226(2):469–476. [PubMed: 20672329]
29. Mosser DM, Edwards JP. Exploring the full spectrum of macrophage activation. *Nature Reviews Immunology*. 2008; 8(12):958–969.
30. Jay SM, Skokos E, Laiwalla F, Krady MM, Kyriakides TR. Foreign body giant cell formation is preceded by lamellipodia formation and can be attenuated by inhibition of Rac1 activation. *American Journal of Pathology*. 2007; 171(2):632–640. [PubMed: 17556592]
31. Chow JC, Young DW, Golenbock DT, Christ WJ, Gusovsky F. Toll-like receptor-4 mediates lipopolysaccharide-induced signal transduction. *Journal of Biological Chemistry*. 1999; 274(16):10689–10692. [PubMed: 10196138]
32. Gordon S. Macrophage heterogeneity and tissue lipids. *Journal of Clinical Investigation*. 2007; 117(1):89–93. [PubMed: 17200712]
33. Backe E, Schwarting R, Gerdes J, Ernst M, Stein H. Ber-mac3 - new monoclonal-antibody that defines human monocyte macrophage differentiation antigen. *Journal of Clinical Pathology*. 1991; 44(11):936–945. [PubMed: 1721628]
34. Dvir T, Timko BP, Kohane DS, Langer R. Nanotechnological strategies for engineering complex tissues. *Nature Nanotechnology*. 2011; 6(1):13–22.
35. Hubbell JA. Biomaterials in tissue engineering. *Bio-Technology*. 1995; 13(6):565–576. [PubMed: 9634795]
36. Sreejalekshmi KG, Nair PD. Biomimeticity in tissue engineering scaffolds through synthetic peptide modifications-Altering chemistry for enhanced biological response. *Journal of Biomedical Materials Research Part A*. 2011; 96A(2):477–491. [PubMed: 21171167]
37. Hern DL, Hubbell JA. Incorporation of adhesion peptides into nonadhesive hydrogels useful for tissue resurfacing. *Journal of Biomedical Materials Research*. 1998; 39(2):266–76. [PubMed: 9457557]
38. Graves KL, Roman J. Fibronectin modulates expression of interleukin-1 beta and its receptor antagonist in human mononuclear cells. *American Journal of Physiology-Lung Cellular and Molecular Physiology*. 1996; 271(1):L61–L69.
39. Simms HH, Damico R, Bland KI. Integrin stimulation regulates polymorphonuclear leukocytes inflammatory cytokine expression. *Annals of Surgery*. 1997; 225(6):757–763. [PubMed: 9230816]
40. Erickson, CAR. *Clinical Immunology*. Baltimore: Williams & Wilkins; 1989.
41. Ruoslahti E. RGD and other recognition sequences for integrins. *Annual Review of Cell And Developmental Biology*. 1996; 12:697–715.
42. McNally AK, MacEwan SR, Anderson JM. alpha subunit partners to beta 1 and beta 2 integrins during IL-4-induced foreign body giant cell formation. *Journal of Biomedical Materials Research Part A*. 2007; 82A(3):568–574. [PubMed: 17311314]
43. Kao WJ, Lee D, Schense JC, Hubbell TA. Fibronectin modulates macrophage adhesion and FBGC formation: The pole of RGD, PHSRN, and PRRARV domains. *Journal of Biomedical Materials Research*. 2001; 55(1):79–88. [PubMed: 11426401]

44. McNally AK, Anderson JM. beta 1 and beta 2 integrins mediate adhesion during macrophage fusion and multinucleated foreign body giant cell formation. *American Journal Of Pathology*. 2002; 160(2):621–630. [PubMed: 11839583]
45. Collie AMB, Bota PCS, Johns RE, Maier RV, Stayton PS. Differential monocyte/macrophage interleukin-1 beta production due to biomaterial topography requires the beta 2 integrin signaling pathway. *Journal of Biomedical Materials Research Part A*. 2011; 96A(1):162–169. [PubMed: 21105164]
46. Ung DY, Woodhouse KA, Sefton MV. Tumor necrosis factor (TNF alpha) production by rat peritoneal macrophages is not polyacrylate surface-chemistry dependent. *Journal of Biomedical Materials Research*. 1999; 46(3):324–330. [PubMed: 10397988]
47. Luttikhuisen DT, Harmsen MC, Van Luyn MJA. Cellular and molecular dynamics in the foreign body reaction. *Tissue Engineering*. 2006; 12(7):1955–1970. [PubMed: 16889525]
48. Gretzer C, Emanuelsson L, Liljensten E, Thomsen P. The inflammatory cell influx and cytokines changes during transition from acute inflammation to fibrous repair around implanted materials. *Journal of Biomaterials Science-Polymer Edition*. 2006; 17(6):669–687. [PubMed: 16892728]
49. Higgins DM, Basaraba RJ, Hohnbaum AC, Lee EJ, Grainger DW, Gonzalez-Juarrero M. Localized Immunosuppressive Environment in the Foreign Body Response to Implanted Biomaterials. *American Journal of Pathology*. 2009; 175(1):161–170. [PubMed: 19528351]
50. Lynn AD, Bryant SJ. Phenotypic changes in bone marrow-derived murine macrophages cultured on PEG-based hydrogels activated or not by lipopolysaccharide. *Acta Biomaterialia*. 2011; 7(1): 123–132. [PubMed: 20674808]
51. Bota PCS, Collie AMB, Puolakkainen P, Vernon RB, Sage EH, Ratner BD, Stayton PS. Biomaterial topography alters healing in vivo and monocyte/macrophage activation in vitro. *Journal of Biomedical Materials Research Part A*. 95A(2):649–657.
52. Knight PT, Kirk JT, Anderson JM, Mather PT. In vivo kinetic degradation analysis and biocompatibility of aliphatic polyester polyurethanes. *Journal of Biomedical Materials Research Part A*. 2010; 94A(2):333–343. [PubMed: 20583334]
53. Cao HQ, McHugh K, Chew SY, Anderson JM. The topographical effect of electrospun nanofibrous scaffolds on the in vivo and in vitro foreign body reaction. *Journal of Biomedical Materials Research Part A*. 2010; 93A(3):1151–1159. [PubMed: 19768795]
54. Keselowsky BG, Bridges AW, Burns KL, Tate CC, Babensee JE, LaPlaca MC, Garcia AJ. Role of plasma fibronectin in the foreign body response to biomaterials. *Biomaterials*. 2007; 28(25):3626–3631. [PubMed: 17521718]
55. Wang N, Tolic-Norrelykke IM, Chen JX, Mijailovich SM, Butler JP, Fredberg JJ, Stamenovic D. Cell prestress. I. Stiffness and prestress are closely associated in adherent contractile cells. *American Journal of Physiology-Cell Physiology*. 2002; 282(3):C606–C616. [PubMed: 11832346]
56. Fereol S, Fodil R, Laurent VM, Balland M, Louis B, Pelle G, Henon S, Planus E, Isabey D. Prestress and Adhesion Site Dynamics Control Cell Sensitivity to Extracellular Stiffness. *Biophysical Journal*. 2009; 96(5):2009–2022. [PubMed: 19254561]
57. Hoffman BD, Grashoff C, Schwartz MA. Dynamic molecular processes mediate cellular mechanotransduction. *Nature*. 475(7356):316–323. [PubMed: 21776077]
58. Jones GE, Allen WE, Ridley AJ. The Rho GTPases in macrophage motility and chemotaxis. *Cell Adhesion and Communication*. 1998; 6(2–3):237–245. [PubMed: 9823474]
59. Teoh SH. Fatigue of biomaterials: a review. *International Journal of Fatigue*. 2000; 22(10):825–837.
60. Bryant SJ, Anseth KS. Hydrogel properties influence ECM production by chondrocyte photoencapsulated in poly(ethylene glycol) hydrogels. *Journal of Biomedical Materials Research*. 2001; 59:63–72. [PubMed: 11745538]
61. Burdick JA, Anseth KS. Photoencapsulation of osteoblasts in injectable RGD-modified PEG hydrogels for bone tissue engineering. *Biomaterials*. 2002; 23(22):4315–4323. [PubMed: 12219821]
62. Sontjens SHM, Nettles DL, Carnahan MA, Setton LA, Grinstaff MW. Biodendrimer-based hydrogel scaffolds for cartilage tissue repair. *Biomacromolecules*. 2006; 7(1):310–316. [PubMed: 16398530]

63. Nicodemus GD, Skaalure SC, Bryant SJ. Gel structure impacts pericellular and extracellular matrix deposition which subsequently alters metabolic activities in chondrocyte-laden PEG hydrogels. *Acta Biomaterialia*. 2011; 7(2):492–504. [PubMed: 20804868]
64. Lampe KJ, Mooney RG, Bjugstad KB, Mahoney MJ. Effect of macromer weight percent on neural cell growth in 2D and 3D nondegradable PEG hydrogel culture. *Journal of Biomedical Materials Research Part A*. 2010; 94A(4):1162–1171. [PubMed: 20694983]

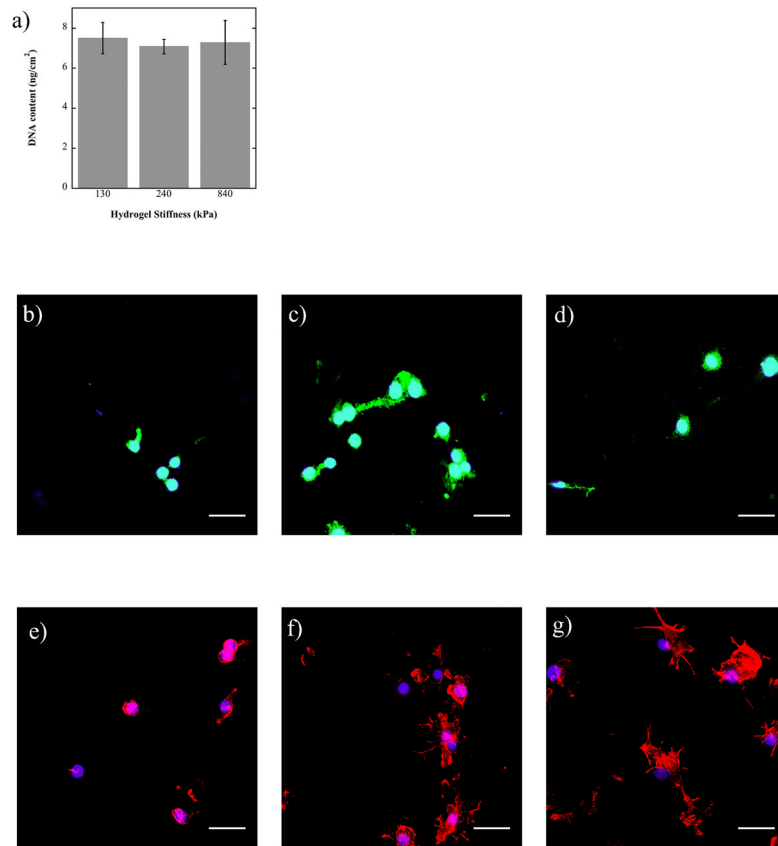


Figure 1.

a) Macrophage (RAW 264.7) attachment, measured by DNA content, after 24 hours *in vitro* when cultured on 130, 240 and 840 kPa PEG-RGD hydrogels (n=4). b–d) Spatial localization of α_v integrins in macrophages (RAW 264.7) cultured on 130 (b), 240 (c), and 840 (e) kPa PEG-RGD gels for 48 hours. e–f) Spatial localization of F-actin in macrophages (RAW 264.7) cultured on 130 (e), 240 (f), and 840 (g) kPa PEG-RGD gels for 48 hours. Nuclei are counterstained with DAPI (blue) (b–g). Scale bar = 32 μ m.

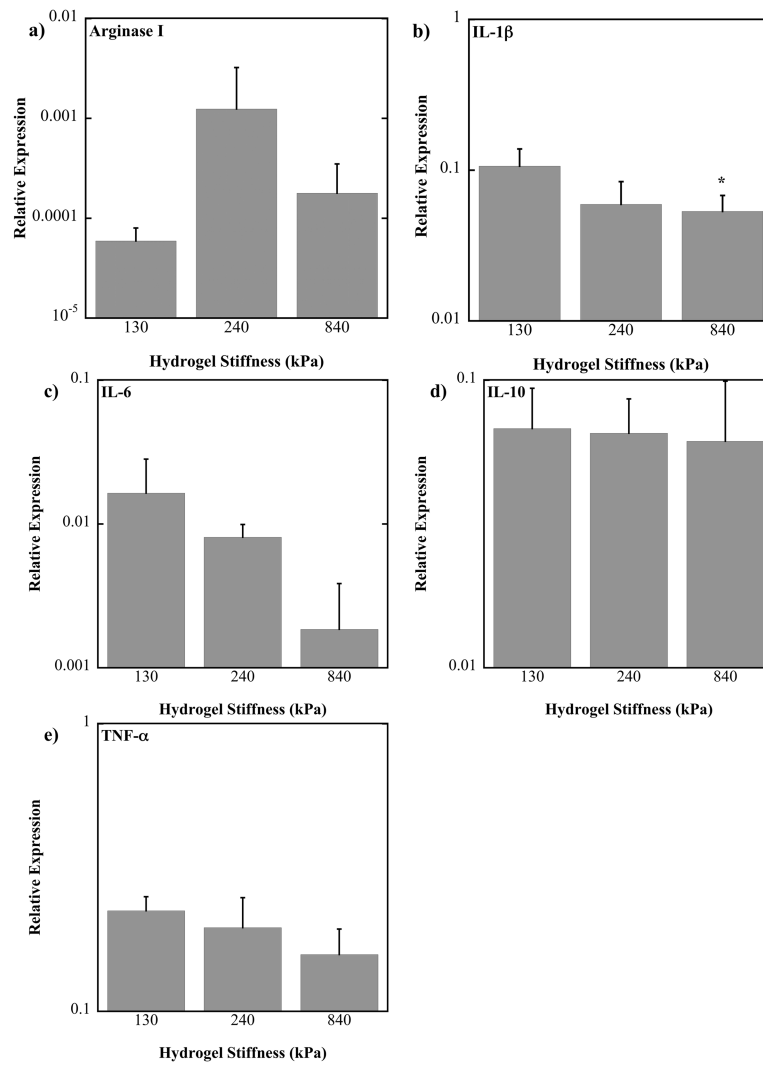


Figure 2. Relative gene expression of murine bone marrow-derived primary macrophages cultured on 130, 240 and 840 kPa PEG-RGD hydrogels for 24 hours. Gene expression is relative to the stable housekeeping gene, L32. * above a bar indicates a significant difference from the 130 kPa level of expression with $p < 0.05$. Note that plots are on a log scale. (n=4).

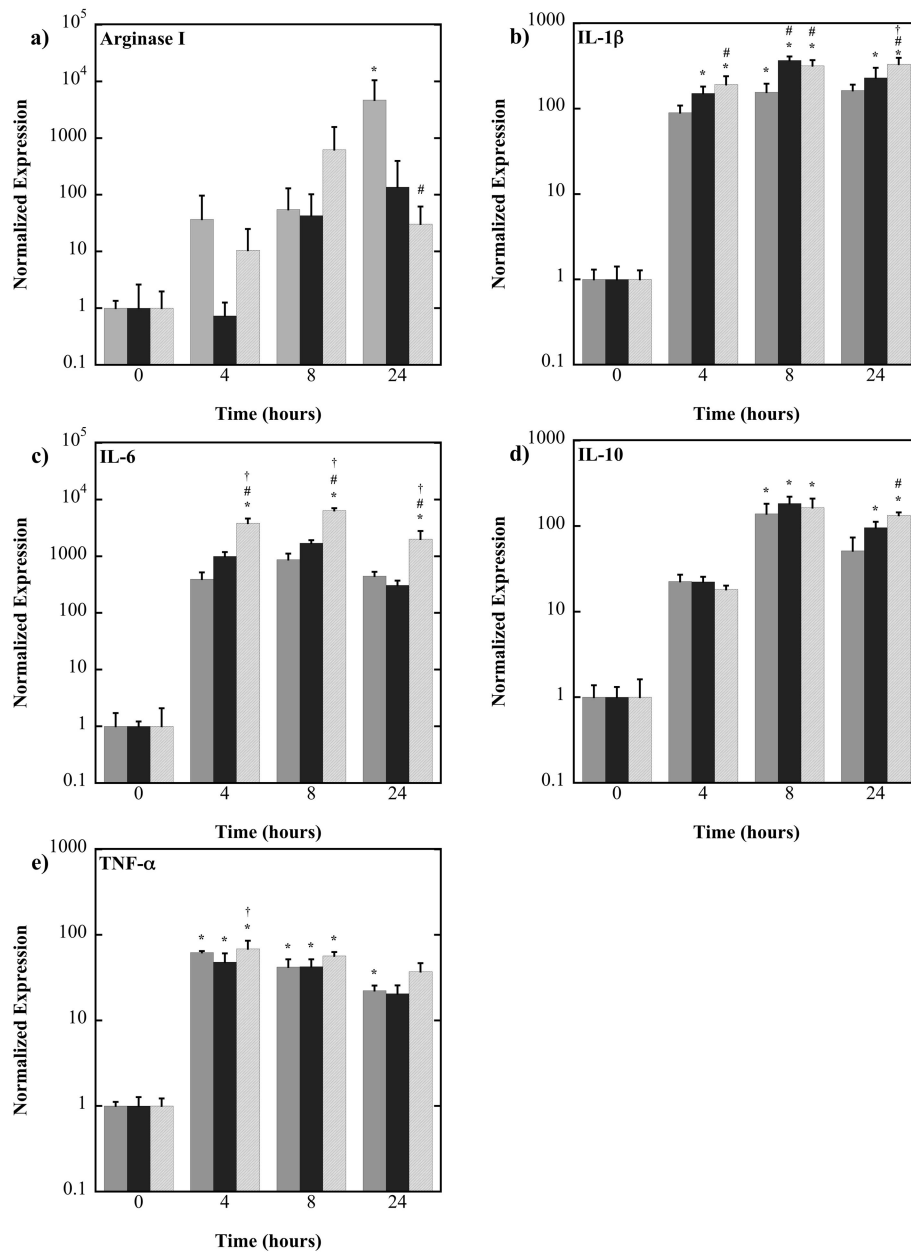


Figure 3. Normalized gene expression of murine bone marrow-derived primary macrophages cultured on 130 (light gray), 240 (dark gray) and 840 (hash mark) kPa PEG-RGD hydrogels in the presence of lipopolysaccharide. Gene expression was normalized to the zero hour time point for each gel stiffness. *above a bar indicate significance from the 0 hour time point of the same gel stiffness, # indicates significance from the 130 kPa hydrogel at the same time point, and † indicates significance from the 240 kPa hydrogel at the same time, $p < 0.05$. Note that plots are on a log scale. (n=4).

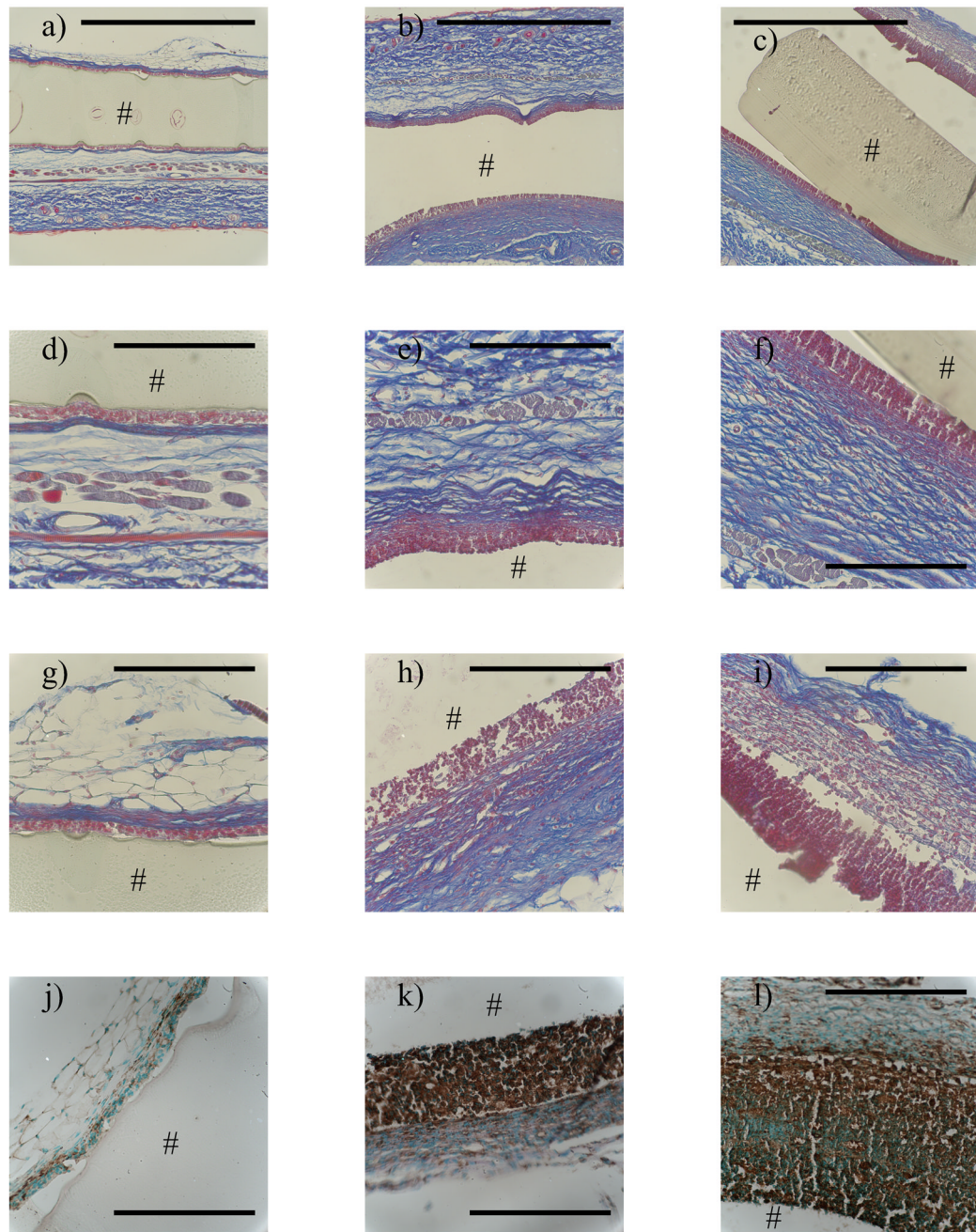


Figure 4. The *in vivo* host response to implanted PEG-RGD hydrogels 28 days post-implantation in subcutaneous pockets of immunocompetent mice: Masson's Trichrome staining (a–i) and Mac3 staining (j–l) for the 130 kPa (a,d,g,j), 240 kPa (b,e,h,k) and 840 kPa (c,f,i,l) constructs. 10X images (a,b,c) show both dorsal and ventral side and 40X images show dorsal (d–f) and ventral (g–l) sides. # indicates the location of the hydrogel. Scale bar on 10X image = 1000 μm and on 40X image = 200 μm .

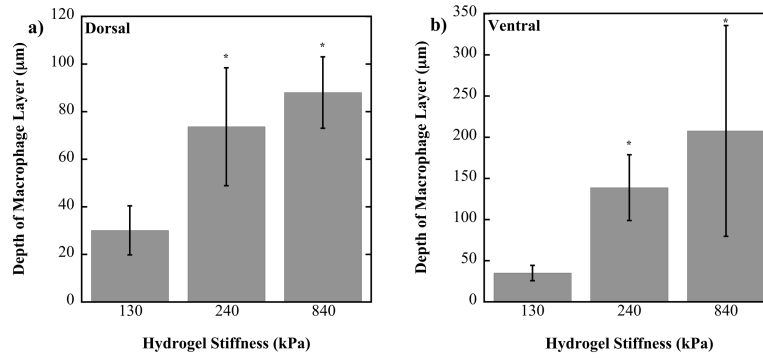


Figure 5. Semi-quantitative analysis of the layer of macrophages around the 130, 240 and 840 kPa PEG-RGD hydrogel implants on the dorsal (a) and ventral (b) sides. * above a bar indicates a significant difference from the 130 kPa construct with $p < 0.05$.

TABLE 1

Material properties of PEG-RGD hydrogels.

| PEG-dA (% w/w) | Tangent modulus (kPa)* | Equilibrium Mass Swelling ratio |
|----------------|------------------------|---------------------------------|
| 10 | 130 +/- 6 | 10 +/- 0.6 |
| 20 | 240 +/- 50 | 8 +/- 0.9 |
| 40 | 840 +/- 60 | 5 +/- 0.4 |

*
under compression

TABLE 2

One-way ANOVA results from relative gene expression.

| Gene of interest | ANOVA factor- Gel stiffness |
|------------------|-----------------------------|
| TNF- α | $p = 0.115$ |
| IL-1 β | 0.028 |
| IL-6 | 0.066 |
| IL-10 | 0.949 |
| Arginase I | 0.358 |

TABLE 3

Two way ANOVA results from normalized gene expression.

| Gene of interest | ANOVA Factor | | |
|------------------|--------------|---------------|-------------|
| | Time | Gel Stiffness | Interaction |
| TNF- α | $p < 0.0001$ | $p < 0.0001$ | $p = 0.113$ |
| IL-1 β | < 0.0001 | < 0.0001 | < 0.0001 |
| IL-6 | < 0.0001 | < 0.0001 | < 0.0001 |
| IL-10 | < 0.0001 | 0.004 | 0.005 |
| Arginase I | 0.136 | 0.246 | 0.096 |